

The Neural and Computational Basis of Controlled Speed–Accuracy Tradeoff during Task Performance

Vincent van Veen^{1,2}, Marie K. Krug², and Cameron S. Carter²

Abstract

■ People are capable, at will, of trading speed for accuracy when performing a task; they can focus on performing accurately at the cost of being slow, or emphasize speed at the cost of decreased accuracy. Here, we used functional magnetic resonance imaging to investigate the neural correlates of this ability. We show increased baseline activity during speed emphasis in a network of areas related to response preparation and execution, including the premotor areas of the frontal lobe, the basal ganglia, the thalamus, and the dorsolateral pre-

frontal and left parietal cortices. Furthermore, speed emphasis was associated with reduced transient response-related activation in several of these structures, suggesting that because of the greater baseline activity under speed emphasis, less activation is needed in these structures to reach response threshold, consistent with the assumptions of several computational theories. Moreover, we identify the dorsolateral prefrontal cortex as providing the top–down control signal that increases this baseline activity. ■

INTRODUCTION

The faster we attempt to perform a task, the greater the chance of making an error; conversely, greater focus on performing accurately comes at the cost of performing more slowly, a phenomenon known as speed–accuracy tradeoff (SAT) (Rinkenauer, Osman, Ulrich, Müller-Gethmann, & Mattes, 2004; Osman et al., 2000; Meyer, Irwin, Osman, & Kounios, 1988; Wickelgren, 1977). The neural basis of the ability to regulate performance between these different strategies is not well understood.

Current psychological models of decision making have generally proposed that responses are based on the accumulation of evidence for one option or another (Bogacz, Brown, Moehlis, Holmes, & Cohen, 2006; Smith & Ratcliff, 2004; Reddi, Asrress, & Carpenter, 2003; Usher & McClelland, 2001; Reddi & Carpenter, 2000; Ratcliff & Rouder, 1998; Pachella, 1974). This is in agreement with neurophysiological and psychophysiological observations (Lo & Wang, 2006; Huk & Shadlen, 2005; Schall, 2003, 2004; Smith & Ratcliff, 2004; Roitman & Shadlen, 2002; Shadlen & Newsome, 2001; Gold & Shadlen, 2000; Hanes & Schall, 1996; Gratton, Coles, & Donchin, 1992; Gratton, Coles, Sirevaag, Eriksen, & Donchin, 1988). Despite their differences, all of these accumulation models share the assumption that, upon stimulus presentation, activity starts to increase from baseline; when a threshold is reached, a decision is made.

A further assumption shared by all of these accumulation models is that SAT can be accounted for by a change in the distance between the baseline and the threshold (Bogacz et al., 2006; Simen, Cohen, & Holmes, 2006; Usher & McClelland, 2001; Reddi & Carpenter, 2000; Ratcliff & Rouder, 1998; Pachella, 1974). Thus, the shorter the baseline–threshold distance, the faster the threshold is reached. This results in a fast reaction time (RT), although this comes at the cost of an increased chance of an error, as small incorrect activations on the basis of noise or irrelevant stimuli might lead the incorrect response to reach the threshold first. Conversely, with a greater baseline–threshold distance, it takes longer to reach the threshold, and small incorrect activations have a smaller chance of reaching threshold first, thus resulting in more accurate but slower performance.

There is, however, no direct evidence that a change in SAT is associated with a change in baseline activity or threshold. Furthermore, it is still unknown how the brain controls SAT. We have attempted to address these issues in the current study using a simple response interference task, the Simon task (e.g., Zorzi & Umiltà, 1995; Craft & Simon, 1970); in this task, participants are asked to respond to the color of a square presented to the left or right of fixation, and ignore the location. A basic simple parallel distributed processing (PDP; see Rumelhart, McClelland, & the PDP Research Group, 1986) model capable of SAT in this task is presented in Figure 1A. This model is similar to the model of the Simon task proposed by Zorzi and Umiltà (1995) and is based on the general

¹University of Pittsburgh, ²University of California, Davis

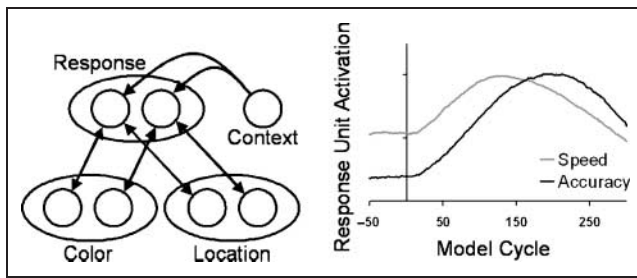


Figure 1. Connectionist model of the Simon task capable of SAT. (A) Architecture of the model. (B) Time course of activation of the correct response unit under speed (gray) and accuracy (black) emphasis. Target stimulus onset occurs at cycle 0. Speed emphasis is achieved by externally setting the context unit to a high level of activity in a sustained fashion. This increases the baseline activity of the response units, as seen in the increased prestimulus baseline. As a result, less activity is needed to reach the response threshold, resulting in a fast RT. In contrast, accuracy emphasis is achieved by low activation of the context unit, which results in a reduced baseline activity of the response layer, so that more activity is needed to reach the threshold. The model is a hybrid of the Simon task model by Zorzi and Umiltà (1995), and the SAT model by Simen et al. (2006). Model results were consistent across a wide range of parameter settings.

architecture proposed by Usher and McClelland (2001) and Cohen, Dunbar, and McClelland (1990). Note, however, that SAT would be implemented in comparable ways in alternative models such as a random walk or diffusion model. The model features two input units for the relevant stimulus dimension (color), two input units for the irrelevant stimulus dimension (location), and two response units. In addition, the model features a “context” unit that is connected to the response units. Changes in this context unit’s level of sustained activity are thus capable of modulating the baseline activity of the response units. As shown in Figure 1B, when the context unit’s activity is set high, the baseline activity of the response units is also high, resulting in a smaller transient activation and speed emphasis; when the context unit’s activity is set low, the baseline activity of the response units is also low, resulting in greater transient activation and accuracy emphasis. Indeed, when the context unit’s activity is set high, the model’s responses are faster but less accurate than when activation of the context unit is low; thus, this model is able to regulate its level of SAT by changes in the sustained activity of its context unit.

Context or task requirements are thought to be represented by the dorsolateral prefrontal cortex (DLPFC) (Miller & Cohen, 2001; Cohen, Servan-Schreiber, & McClelland, 1992). This area is thought to be critically involved in attentional processes by increasing the activation of task-relevant representations in posterior cortices (Egner & Hirsch, 2005; Miller & D’Esposito, 2005; Miller & Cohen, 2001; Cohen et al., 1992). Thus, we hypothesize that the DLPFC regulates the accumulation mechanism underlying SAT by performing a similar function as the context unit in our model displayed in

Figure 1; we hypothesize that the DLPFC provides the top-down signal that increases the baseline activity of the motor representations in the posterior and motor cortex.

The distinction we make here, between the implementation of SAT as a change in the baseline–threshold distance and the control of SAT, is similar to the distinction between the implementation and control of perceptual attention (cf. Miller & Cohen, 2001; Luck & Hillyard, 2000; Desimone & Duncan, 1995). The implementation of attention is thought to involve the amplification of the neural signal related to the processing of the features of the attended stimulus (with the simultaneous reduction of the neural signal related to the features of the ignored stimulus). The control of attention is thought to be dependent on a top-down control signal from the DLPFC. Likewise, we hypothesize that the control of SAT is dependent on a top-down control signal from the DLPFC, whereas the implementation of SAT should occur by a modulation of the baseline–threshold distance, most likely in regions related to decision making and the preparation and execution of responses.

In the present experiment, participants were instructed with cues to emphasize either speed or accuracy in a set of trials that followed each cue (see Figure 2), while performing a simple response interference task, the Simon task (e.g., Craft & Simon, 1970). We predicted that the processing of each cue would lead to a change in sustained baseline activity, which would be measurable with functional magnetic resonance imaging (fMRI). By studying the neural substrates as well as the computational processes they implement, we sought to engage brain areas involved with SAT.

Because increased sustained activity of the context unit in our model results in speed emphasis, we predict that sustained activity of the DLPFC should be greater during speed emphasis than during accuracy emphasis. Furthermore, we predicted that regions associated with decision making and response preparation/execution should also show a greater level of baseline activity during speed emphasis, over and above transient activation to the Simon trials. Conversely, assuming that a greater buildup of neural evidence will lead to an increased blood oxygenation level-dependent (BOLD) response, we predicted these regions’ transient activation to the Simon trials to be greater under accuracy emphasis, as it should require more accumulated evidence to reach a response threshold under accuracy emphasis. Thus, we predicted that for areas involved with making decisions and preparing and executing responses, speed emphasis will increase the sustained baseline activity, while at the same time reducing transient activation (see Figure 3). Finally, we predict that functional connectivity between the DLPFC and the regions implementing SAT should be increased during speed emphasis compared to accuracy emphasis.

METHODS

Participants

Twenty healthy, right-handed adults (10 women; mean age = 25 years) participated in this experiment, after having provided written informed consent in accordance with the IRB of the University of California at Davis.

Task

Participants performed three runs of trials during scanning. The gray outline of two squares was visible throughout each run, along with a fixation point. Each run was divided into several “miniblocks.” Each miniblock started with an instruction cue (a large uppercase “A” or a large uppercase “S”; prior to the experiment, participants were instructed that when they saw an “A,” they were to focus on accuracy during the upcoming trials, and when they saw an “S,” they were to focus on speed during the upcoming trials). This cue lasted 1000 msec, followed by a 5000-msec fixation screen. After cue offset, the center-screen fixation point was changed to a small up-

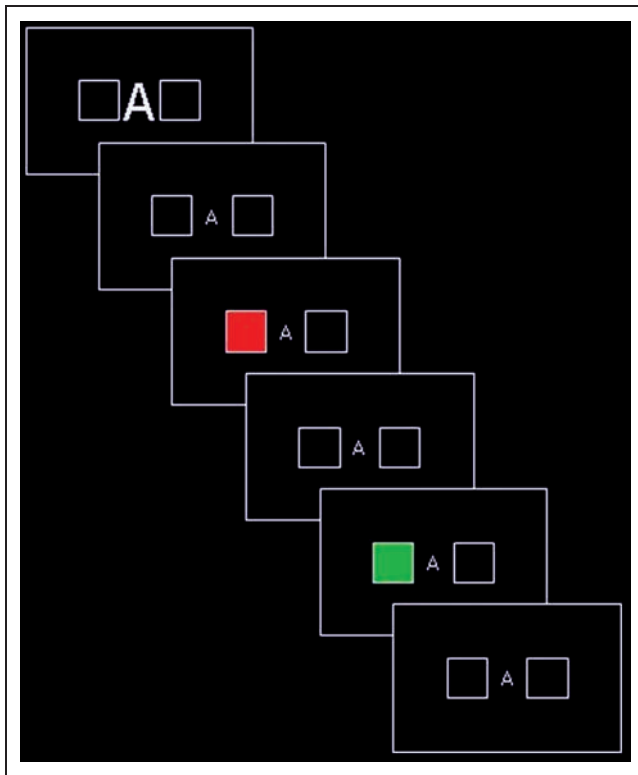


Figure 2. Example of the task. Participants performed a Simon task, during which they had to respond to the color of a square presented to the left or right of fixation with a left or right index finger button press. Participants were presented with either an uppercase “A” (shown in example) or “S,” indicating that they had to emphasize accuracy or speed, respectively, during the subsequent miniblock of Simon trials. Each cue lasted 1000 msec, followed by a 5000-msec fixation screen, after which the miniblock started. Simon trials lasted 3000 msec each; after each miniblock, a 12,000-msec fixation screen appeared to allow for activity to return to resting state.

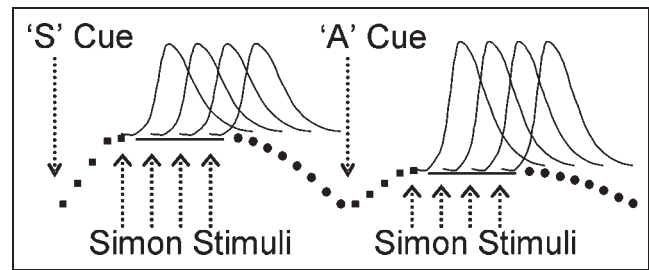


Figure 3. Overview of the predictors used. For our regression analyses, we used the following predictors for speed and accuracy emphasis: 5 postcue, single time-point predictors (squares); a sustained baseline predictor (horizontal lines); 8 post-miniblock, single time-point predictors (circles); HRF-convolved transient predictors for congruent, incongruent, and error trials. For illustrative purposes, the predictors in the figure are scaled according to our predictions: in order to emphasize speed, the sustained baseline should be increased compared to accuracy emphasis, whereas transient, response-related activation should be decreased.

percase “A” or a small uppercase “S.” For each SAT condition (speed and accuracy emphasis), there were seven miniblocks of 4 trials, four miniblocks of 8 trials, and one miniblock of 20 trials within each run. Within each run, these miniblocks were presented in random order. Each run started and ended with a 12-sec fixation screen containing the two squares and the fixation point.

During each Simon trial, one of the squares lit up either green or red for 150 msec, followed by a 2850-msec intertrial interval. The exception was the last stimulus of each miniblock, which was followed by a 14,850-msec fixation screen, after which the next cue was presented (thus, the stimulus onset asynchrony [SOA] from the last stimulus of a miniblock to the next cue was 15,000 msec).

Prior to the experiment, participants were instructed to respond to the color of the square (red or green) with a left or right index finger button press (counter-balanced across participants). Congruent trials (2/3 of all trials) were trials during which the stimulus location and response hand corresponded (e.g., a left stimulus mapped onto the left hand); incongruent trials (1/3 of all trials) were trials during which the stimulus was mapped onto the opposite response hand (e.g., a left stimulus mapped onto the right hand).

fMRI Data Acquisition

Functional images were acquired with a 3-T whole-body MRI system (Siemens AG, Munich, Germany), using T2*-weighted gradient-recalled echo (field of view = 220 mm; matrix = 64 × 64; 28 oblique axial slices; slice thickness = 4.0 mm; TR = 1500 msec; TE = 25 msec; FA = 90°). Data were preprocessed and analyzed using BrainVoyager (Brain Innovation, Maastricht, Netherlands). As each run started with a 12,000-msec fixation screen, the first eight images were discarded from the analysis. The remaining 608 images of each run were preprocessed using interscan

slice time correction, 3-D motion correction, 3-D Gaussian spatial filtering (full width at half maximum = 6 mm), and temporal high-pass filtering using a low cutoff frequency of 3 cycles/run. For each participant, three-dimensional images (magnetization prepared rapid gradient echo, MP-RAGE) of the brain were acquired at the end of the experiment; functional data were aligned to these images and then transformed into Talairach space.

fMRI Data Analysis

Multiple regression was performed, using participant as a random factor, with separate sets of regressors for the baseline activity and the transient activation under speed and accuracy emphasis. In order to identify transient activation to the Simon stimuli, we used regressors convolved with a generic hemodynamic response function (HRF) locked to the Simon stimuli, separately for the congruent, incongruent, and error trials, and for speed and accuracy emphasis. Additionally, in order to identify differences in sustained baseline activity, we used a sustained baseline regressor accounting for the baseline activity throughout each miniblock, and 13 single time-point regressors accounting for the first five scans following the presentation of a cue and the last eight scans of each miniblock (corresponding to the fixation screen), for both speed and accuracy emphasis. This approach is comparable to a hybrid blocked/event-related design (Dosenbach et al., 2006; Visscher et al., 2003). An illustration of the regressors used (scaled according to our predictions for illustrative purposes) is depicted in Figure 3. In all analyses reported, temporal autocorrelation in the fMRI time series was corrected using an autoregressive function.

The obtained beta weights (parameter estimates) for these regressors were then subjected to second-level analyses. Voxelwise paired *t* tests between the estimated beta weights for the “sustained baseline” regressors for the speed and accuracy conditions were used to identify regions whose baseline activity differed between speed and accuracy emphasis, using a per-voxel statistical threshold of $p < .001$ (two-tailed, uncorrected), and a contiguity threshold of 350 mm³.

To investigate possible differences between baseline activity under speed and accuracy emphasis throughout each miniblock (over and above the transient responses each area might have to the Simon trials), two types of post hoc analyses were performed on the average signal of each of the identified areas. First, any area that would differentially raise its baseline activity in response to the cues would show a greater increase in activation following the presentation of the cue. Thus, we performed a random effects analysis of variance (ANOVA) using SAT (speed, accuracy) and time point (the five single time-point estimates following the presentation of each cue) as factors. Second, any area that increased its baseline activity would show a greater drop-off of activity at the

offset of each miniblock. We therefore performed a random effects ANOVA using SAT (speed, accuracy) and time point (the eight single time-point estimates at the end of each miniblock) as factors.

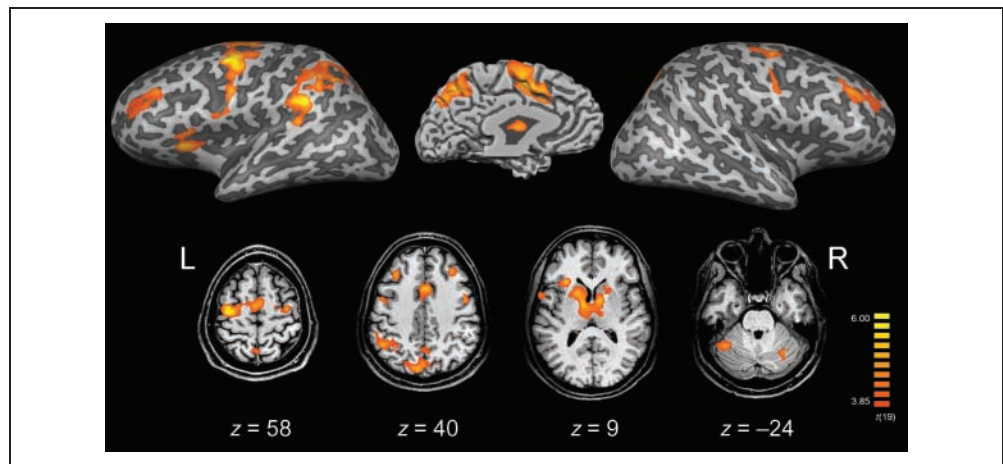
In order to assess possible differences in transient activation under speed and accuracy emphasis, per-participant beta weights obtained for congruent and incongruent conditions were subjected to a condition by SAT repeated-measures ANOVA; regions showing increased transient activation under one or other condition would be identified by a significant main effect of SAT.

To further assess whether activation related to making an overt response was greater under accuracy emphasis, we deconvolved the fMRI signal from the obtained regions (averaged across voxels and *z*-scored). A deconvolution analysis is one that estimates each time point of the hemodynamic response following a particular event, without using an explicit model of the hemodynamic response itself (Glover, 1999). In addition to the regressors accounting for baseline activity, the regressors used for these analyses included eight time points following each Simon stimulus (and error trials as regressors of noninterest), separate for speed and accuracy emphasis. We then averaged the obtained signal across congruent and incongruent regressors to obtain an estimate of the BOLD response under speed and accuracy emphasis for each of the observed regions. To test whether this activation differed between speed and accuracy emphasis, we subtracted Scan 1 from the peak (Scan 3, 4, or 5), and performed paired *t* tests for each region.

We analyzed response-related activation of the engaged dorsal premotor regions by deconvolving the fMRI signal for correct left- and right-hand responses using eight time points (in addition to regressors accounting for baseline activity and error trials). We then averaged contralateral responses for the left and right dorsal premotor cortex (PMC) (activation in the left dorsal PMC was separated from the medial wall activation by raising the threshold until the activation separated into two separate regions, one on the lateral dorsal PMC and one in the supplementary motor area [SMA]/anterior cingulate cortex [ACC]). Again, to test whether this activation differed between speed and accuracy emphasis, we subtracted the peak (Scan 3 or 4) from Scan 1 and performed a paired *t* test.

To test whether the DLPFC does indeed have a top-down influence on the motor system in the regulation of SAT, we analyzed functional connectivity by conducting psychophysiological interaction (PPI) analyses (Friston et al., 1997). A PPI analysis tests for voxels that show a significant interaction between the time course of a seed region of interest (ROI) and a psychological regressor. The logic of this approach is that when two regions both respond similarly to a psychological manipulation, there will be a correlation between the two areas, but not necessarily a causal relationship. However, when an area shows a significant interaction between the time course of a seed ROI and a psychological regressor, we can assume that this

Figure 4. Cortical and subcortical areas with a difference in sustained baseline activity as identified by a random effects analysis ($p < .001$, uncorrected). (Top, left) Cortical changes in baseline activity displayed on the inflated cortical surface of the left hemisphere of one participant, lateral view. (Top, right) Cortical changes in baseline activity displayed on the inflated cortical surface of the right hemisphere of that same participant, lateral view. (Top, middle) Cortical changes in baseline activity on the medial surface of the left hemisphere. (Bottom) Axial slices displaying activity changes (neurological convention, i.e., left = left) at Talairach $z = 58, 40, 9,$ and -24 .



region's response to the psychological manipulation is modulated by the level of activation of the seed ROI.

Thus, a PPI analysis (Friston et al., 1997) requires a “psychological” regressor, a “physiological” regressor, and their interaction term. The time course of each of the DLPFC ROIs (averaged across voxels and z -scored) was used as physiological regressor; separate PPI analyses were conducted using the left and right DLPFC signal. Miniblock-level psychological regressors were constructed for each participant encoding for the difference between speed and accuracy miniblocks (contrast-coded, with 1 for speed miniblocks and -1 for accuracy miniblocks). For each participant, the product between these two regressors was calculated. Because we hypothesized that in motor/decision regions, the baseline activity should be modulated over and above transient activation to the Simon stimuli, HRF-convolved Simon-locked regressors were also included as regressors of noninterest. Regression analyses were then conducted, once for each of the two DLPFC ROIs. Areas that responded to the PPI term were next identified by testing the per-voxel estimated beta weight for the interaction term against 0, thresholded at $p < .001$ (uncorrected).

Additional similar PPI regression analyses were performed excluding the transient HRF-convolved Simon-locked regressors; however, the results of these analyses did not appear to differ much from the initial PPI analyses. Therefore, only the results of the analyses that included the transient regressors are discussed.

RESULTS

Performance Data

The different conditions yielded the following RTs: congruent speed, 466 msec ($SD = 116$); incongru-

ent speed, 522 msec ($SD = 120$); congruent accuracy, 547 msec ($SD = 104$); incongruent accuracy, 587 msec ($SD = 100$). Error rates to the different conditions were: congruent speed, 3.1% ($SD = 2$); incongruent speed, 12.7% ($SD = 9$); congruent accuracy, 1.4% ($SD = 2$); incongruent accuracy, 4.6% ($SD = 3$). Analysis of the performance data by means of SAT (speed, accuracy) by condition (congruent, incongruent) repeated measures ANOVAs showed that performance was faster [$F(1, 19) = 7.64, p = .012$] but less accurate [$F(1, 19) = 29.90, p < .001$] under speed than under accuracy emphasis, showing that participants did indeed trade speed and accuracy. Main effects of condition verified the standard Simon effect; participants were faster [$F(1, 19) = 94.34, p < .001$] and made fewer errors [$F(1, 19) = 29.74, p < .001$] to congruent than to incongruent trials. Significant interactions between these two factors for both RTs [$F(1, 19) = 12.25, p = .002$] and error rates [$F(1, 19) = 14.41, p = .001$] showed that the Simon effect was greater under speed emphasis. Error RTs were faster than correct RTs [$F(1, 19) = 2.74, p = .013$], although we did not observe significant differences between error RTs under speed and accuracy emphasis. For incongruent trials, error RTs were faster than correct RTs [$t(19) = 6.07, p < .001$]; significant differences between error and correct RTs to congruent trials were not observed.

Neuroimaging Data

Voxelwise paired t tests between the parameter estimates for the speed and accuracy sustained baseline regressors revealed a distributed network of cortical and subcortical areas generally thought to be involved with making decisions and planning and executing responses (see Figure 4). These encompassed the bilateral DLPFC

Table 1. Areas Whose Sustained Baseline Activity Differs between Speed and Accuracy Emphasis

Brain Region	Volume (mm ³)	Talairach Coordinates			BA
		x	y	z	
Left DLPFC	1179	-33	34	35	8/9/46
Right DLPFC	625	33	34	39	8/9
ACC/SMA/left PMC	16578	-15	-4	53	6/32/24
left PMC	3446	-31	-11	57	6
ACC/SMA	4162	0	1	53	32/24
Right dorsal PMC	576	34	-10	55	6
Right dorsal PMC	499	47	1	42	6
Left ventral PMC	819	-54	9	7	6
Left anterior Insula	1313	-31	21	11	
Left IPL/supramarginal gyrus	6584	-45	-48	40	7/40/22
Precuneus	7056	-3	-68	44	7/19
Basal ganglia/thalamus	13,387	-2	0	9	
Left cerebellum	1555	-40	-50	-25	
Right cerebellum	448	29	-62	-22	

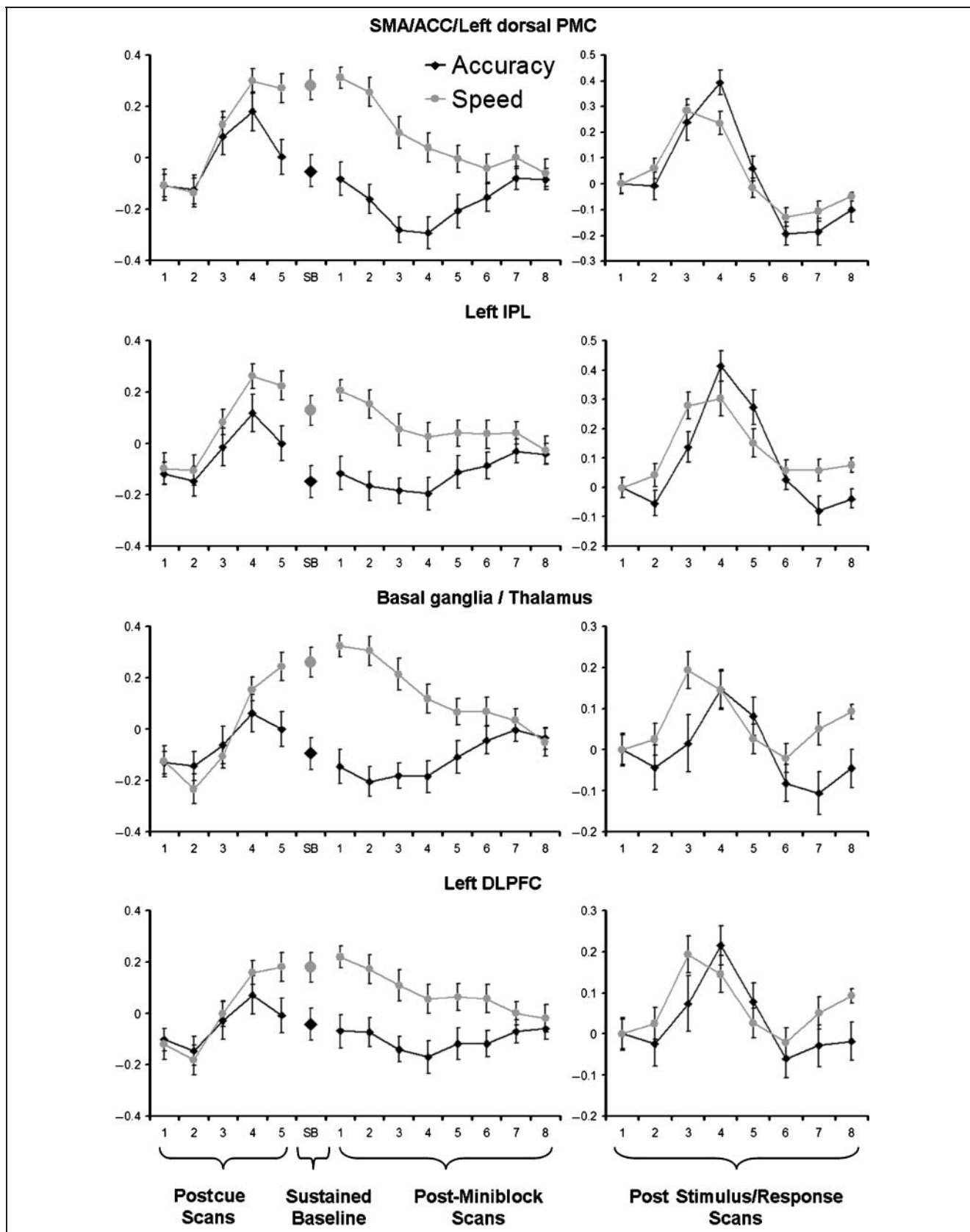
and premotor areas in the frontal lobe, including the dorsal PMC, SMA, and ACC, which are all known to be involved in the preparation and execution of movements (Picard & Strick, 1996, 2001; Ball et al., 1999; Ghez, 1991). Differences were also observed in the left inferior parietal lobule (IPL) including the supramarginal gyrus, and in the left anterior insula. Finally, an increase in baseline activity under speed emphasis was observed in the thalamus (including the dorsomedial, ventrolateral, anterior, and ventral anterior nuclei) and the basal ganglia (including the bilateral caudate nucleus, putamen, and pallidum), and in the bilateral cerebellum, which have also been associated with motor processes (Strick, 2004; Grodd, Hülsmann, Lotze, Wildgruber, & Erb, 2001; Graybiel, Aosaki, Flaherty, & Kimura, 1994). These areas are summarized in Table 1. In each of these areas, speed cues induced greater sustained baseline activity than accuracy cues; no areas were found that displayed the opposite pattern of results.

Representative time courses of baseline activity of four regions are shown in Figure 5, left (medial wall extending into the left dorsal PMC; left IPL; basal ganglia/thalamus; left DLPFC). The time courses of the other areas looked remarkably similar. As can be seen, following the presen-

tation of the cue, there is a greater increase in baseline activity following speed cues than following accuracy cues; furthermore, activity drops off more following a speed miniblock than following an accuracy miniblock. Post hoc analyses of the five single time-point regressors following each cue revealed that this greater increase of activity following speed cues was significant for almost all of the activated regions [SAT by Time-point interaction, $F(4, 76)$ range = 2.51–7.93, all $ps < .05$], the exceptions being the left anterior insula and the left ventral PMC, both of which only showed a trend toward significance [$F(4, 76)$ range = 2.27–2.28, all $ps < .07$]. Likewise, post hoc analyses of the eight single time-point regressors at the end of each miniblock revealed that the activity for almost all of the activated areas decreased more following speed miniblocks than following accuracy miniblocks [SAT by Time-point interaction, $F(7, 133)$ range = 2.21–14.53, all $ps < .05$], the exception being (again) the left ventral PMC, where this interaction failed to reach significance [$F(4, 76) = 1.51, p = .17$].

Because we predicted that areas that show greater sustained baseline activity under speed emphasis should also display smaller transient activation under speed emphasis, random effects ANOVAs were performed using the

Figure 5. Time courses of the activation of four representative regions (SMA/ACC/left dorsal PMC, left IPL, basal ganglia/thalamus, and left DLPFC). (Left) Time course of baseline activity under speed and accuracy emphasis. As can be seen, baseline activity was greater for each area under speed emphasis (gray) than under accuracy emphasis (black). Error bars represent 1 standard error of the mean. SB = sustained baseline. (Right) Deconvolution analyses of activation elicited by the Simon stimuli. Transient, baseline-to-peak activation is greater under accuracy emphasis (black) than under speed emphasis (gray). Note that this transient activation is additive to the sustained baseline activity. Error bars represent 1 standard error of the mean.



transient, hemodynamic regressors on the average signal of each of the regions identified earlier by the comparison between sustained baseline regressors. Significant main effects of SAT showed that transient activation was greater under accuracy than under speed emphasis in the basal ganglia/thalamus, the bilateral dorsal PMC, the left IPL, the precuneus, and the left cerebellum [$F(1, 19)$ range = 4.43–8.12, all $ps < .05$]. A trend toward significance was observed in the ACC/SMA [$F(1, 19) = 3.50$, $p = .08$]. Curiously, a voxelwise random effects ANOVA using the transient, HRF-convolved regressors did not result in any significant main effects of SAT at the chosen threshold ($p = .001$); at a reduced threshold ($p = .005$), activation was observed that was encompassed by the areas identified by the sustained baseline comparison. In short, no regions were observed that showed reduced transient activation under speed emphasis without also showing increased baseline activity under speed emphasis. This continued to be the case when two additional covariates of noninterest were included to account for the trials immediately following errors (under speed and accuracy emphasis); transient activation in the basal ganglia/thalamus, the bilateral dorsal PMC, the left IPL, the precuneus, and the left cerebellum was still greater under accuracy emphasis than under speed emphasis [$F(1, 19)$ range = 5.45–9.34, all $ps < .05$], whereas the ACC/SMA still showed a trend toward significance [$F(1, 19) = 3.57$, $p = .07$].

It is possible that the BOLD response differs between speed and accuracy emphasis conditions, and that, as such, the results of the previous analyses were an artifact of the possibility that the generic HRF we used simply was a better fit for the BOLD function under accuracy emphasis than under speed emphasis. We addressed this potential confound by computing a deconvolution analysis for each ROI obtained in the speed versus accuracy baseline comparison, and comparing the peaks of the obtained estimated BOLD response. For some ROIs, this peak occurred at Time Point 4 under both speed and accuracy emphasis (right dorsal PMC; left ventral PMC; left IPL); however, for other ROIs, the peak under speed emphasis occurred at Time Point 3 (basal ganglia/thalamus; precuneus; bilateral DLPFC; left insula; left and medial premotor regions). For the left and right cerebellum, the peak of the BOLD response occurred at Time Point 5 under both speed and accuracy emphasis.

Results of these analyses indicated that for the bilateral dorsal PMC, the ACC/SMA, the right DLPFC, the bilateral cerebellum, and the left IPL, transient response-related activation was greater under accuracy than under speed emphasis [$t(19)$ range = 2.17–3.10, all $ps < .05$]. However, for the left DLPFC, the left insula, the left ventral PMC, and the basal ganglia/thalamus, this failed to reach significance [$t(19)$ range = .09–1.64, all $ps > .1$]. Comparison of the sustained baseline regressors for speed and accuracy emphasis showed that for almost all ROIs, sustained baseline activity continued to be significantly higher under speed than under accuracy [$t(19)$

range = 2.20–3.19, all $ps < .05$]. For the left ventral PMC, this difference approached significance [$t(19) = 2.07$, $p = .052$]. Thus, in sum, results of the deconvolution analyses, for the most part, replicated the results of the previous analyses using HRF-convolved regressors; transient activation of the lateral and medial premotor regions, the left IPL, and the cerebellum was greater under accuracy than under speed emphasis. Interestingly, however, the basal ganglia/thalamus and the right DLPFC showed different results; transient activation of the basal ganglia/thalamus did not differ between speed and accuracy emphasis according to the deconvolution analyses, whereas activation of the right DLPFC did.

We next attempted a response-specific deconvolution analysis of the bilateral dorsal PMC ROIs (see Methods). This analysis also showed transient response-related activation of the PMC contralateral to the response to be greater under accuracy than under speed emphasis [$t(19) = 2.10$, $p = .050$; see Figure 6].

Results of the PPI analyses are shown in Figure 7 and are summarized in Table 2. Analyses using the left DLPFC as seed region resulted in a network of regions that largely overlapped with those identified in the speed–accuracy sustained baseline comparison described earlier. These regions included the bilateral dorsal PMC, the SMA/ACC, the left IPL, the left anterior insula, and the left thalamus; unique to this analysis was a region in the right posterior inferior frontal gyrus. The analysis using the right DLPFC as seed region resulted in activation of the SMA/ACC and the left dorsal PMC, overlapping with the regions identified by the left DLPFC PPI analysis.

The results of the PPI analyses suggest that the DLPFC controls SAT by increasing the baseline activity in motor-related and decision-related brain regions, and is not related to perceptual attention. To provide further support for this notion, we correlated the differences

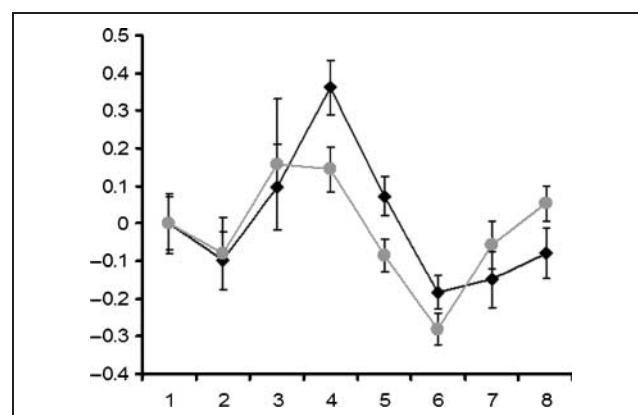
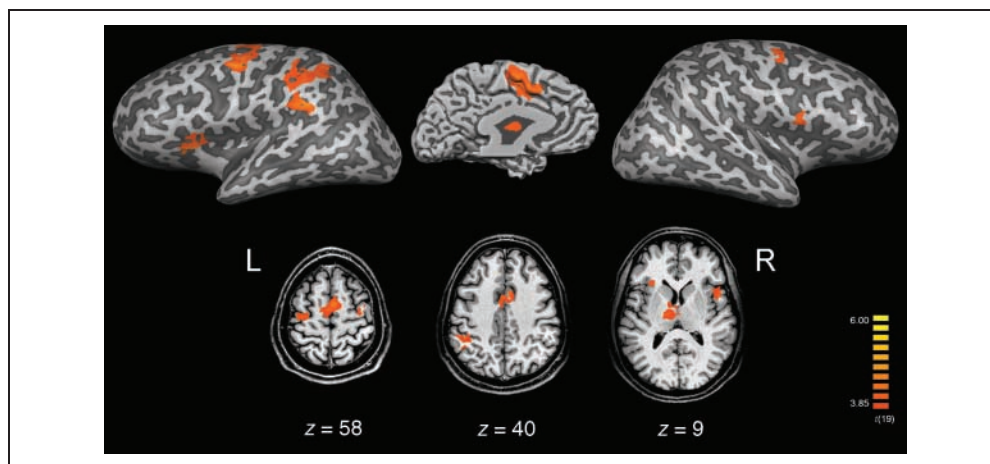


Figure 6. Deconvolved time course of response-related activation of the dorsal premotor cortex, contralateral to the response hand, averaged across the left and right dorsal PMC. This response-related activation was greater under accuracy than under speed emphasis. Error bars represent 1 standard error of the mean.

Figure 7. Results of the PPI analysis using the left DLPFC ($p < .001$, uncorrected). (Top, left) Cortical changes in baseline activity displayed on the inflated cortical surface of the left hemisphere of one participant, lateral view. (Top, right) Cortical changes in baseline activity displayed on the inflated cortical surface of the right hemisphere of that same participant, lateral view. (Top, middle) Cortical changes in baseline activity on the medial surface of the left hemisphere. (Bottom) Axial slices displaying activity changes (neurological convention, i.e., left = left) at Talairach $z = 58$, 40, and 9.



in baseline activity with differences in performance. It could be argued, after all, that the DLPFC in this experiment works to prevent further impaired performance under speed emphasis. The notion that the DLPFC increases baseline activity in motor and decision networks predicts a positive relationship between the increase in baseline activity and the increase in error rates from accuracy to speed emphasis. In contrast, the notion that the DLPFC exerts perceptual attention to prevent further impairment of performance predicts a negative relationship between the increase in baseline activity and the increase in error rates from accuracy to speed emphasis. We tested this by performing a median split on the per-

subject difference in error rates (speed – accuracy) and seeing whether those with a greater difference in error rates would display a greater or a smaller difference in DLPFC sustained activity. Because the PPI analyses suggested that both regions of the DLPFC provide a top-down signal onto the motor and decision networks to control SAT, we averaged across the two areas of the DLPFC. Those with a greater difference in error rates between SAT conditions displayed a greater difference in sustained baseline activity [$t(18) = 2.37$, $p = .029$], suggesting that the increased baseline activity in the DLPFC reflects the control of SAT rather than the control of perceptual attention [for RTs, although in the

Table 2. Areas that are Functionally Connected to the Left and Right DLPFC in Regulating SAT

Brain Region	Volume (mm^3)	Talairach Coordinates			BA
		x	y	z	
<i>Left DLPFC</i>					
Left dorsal PMC	2083	-32	-14	55	6
Right dorsal PMC	423	35	-7	55	6
ACC/SMA	7822	1	-1	54	32/24
Right posterior inferior frontal gyrus	993	46	13	7	44/45
Left IPL	660	-38	-47	48	40
Left IPL/supramarginal gyrus	1390	-51	-41	33	40
Thalamus	1930	-9	-11	12	
Left anterior insula	417	-30	20	12	
<i>Right DLPFC</i>					
ACC/SMA	2157	1	0	53	32/24
Left dorsal PMC	459	-32	-14	55	6

same direction, such a relationship was not significant, $t(18) = 1.08, p = .30$].

DISCUSSION

We obtained evidence showing that, when speed is emphasized, the baseline activity is increased in a network of areas related to decision making and response preparation and execution; this sustained baseline is activated to a lesser degree when accuracy is emphasized. Furthermore, these data also show that the transient activation related to making a response is greater under accuracy emphasis in several of these areas. These results support the assumptions made by our model depicted in Figure 1A, and other computational approaches mentioned earlier (Bogacz et al., 2006; Smith & Ratcliff, 2004; Usher & McClelland, 2001; Ratcliff & Rouder, 1998; Pachella, 1974). As discussed earlier, these models assume that the distance between baseline and threshold is reduced during speed emphasis, such that less activation is needed to reach the response threshold. Note, in particular, the similarity between the activation of the model's correct response unit (Figure 1, right) and the activation of the dorsal PMC (Figure 5B). Thus, these data provide (to our knowledge, the first) supportive evidence for the notion that SAT is indeed implemented as a modulation of this baseline–threshold distance, and have identified the areas involved with this process.

The engagement of cortical and subcortical premotor networks, rather than sensory regions, indicates that the locus of SAT is primarily at the representational level of response preparation (Rinkenauer et al., 2004; Osman et al., 2000); that is, people appear to emphasize speed over accuracy by speeding up response-level processes (rather than stimulus-related processes). Indeed, we did not observe significant differential activations in sensory cortices by the speed and accuracy cues. This is consistent with the assumptions made in our PDP model, and other models (Simen et al., 2006), in which SAT occurs at the response layer. It is also consistent with event-related potential evidence suggesting that controlled SAT influences the response stage during this and comparable tasks (Rinkenauer et al., 2004; Van der Lubbe, Jaśkowski, Wauschkuhn, & Verleger, 2001; Osman et al., 2000).

It is interesting that the left IPL was also influenced by our SAT manipulation, in addition to the premotor areas of the frontal lobe. The parietal areas are often thought to represent stimulus–response mappings (e.g., Bunge, Hazeltine, Scanlon, Rosen, & Gabrieli, 2002). The region engaged by our SAT manipulation might correspond to the lateral intraparietal (LIP) area in the nonhuman primate. A large amount of data has suggested that the LIP is involved with the accumulation of evidence for a sensorimotor decision (Hanks, Ditterich, & Shadlen, 2006; Huk & Shadlen, 2005; Gold & Shadlen, 2002; Roitman & Shadlen, 2002; Shadlen & Newsome, 2001).

Roitman and Shadlen (2002) have shown that a decision is made once the accumulation of evidence in the LIP for one response or another reaches a fixed value, presumably corresponding to a threshold. Although these authors did not experimentally manipulate SAT, they suggested that SAT could be governed by this threshold. In the present data, we did, in fact, observe that SAT modulated both the sustained baseline activity and the transient response-related activation in the left IPL. Our results are thus consistent with the notion that the parietal cortex is involved with SAT. The left lateralization of the parietal area engaged in our study is furthermore consistent with the role of the left parietal cortex in motor attention (Rushworth, Krams, & Passingham, 2001; Rushworth, Paus, & Sipila, 2001).

Two recent studies involving nonhuman primates further support our findings of increased baseline activity in premotor and parietal areas when preparing for speed compared to accuracy. In one study, monkeys were trained to make either slow or fast reach movements; it was found that preparatory activity in the premotor and motor cortices was greater when monkeys prepared to make fast as opposed to slow reach movements (Churchland, Santhanam, & Shenoy, 2006). A second study found that preparatory activity in the parietal reach region predicted the speed of subsequent reach movements (Snyder, Dickinson, & Calton, 2006). Although neither of these two studies explicitly manipulated SAT, it is clear that these findings are convergent with ours.

It has been argued that both the DLPFC and the premotor regions of the frontal lobe engaged in the present study form segregated cortico-striato-thalamo-cortical circuits (Strick, 2004; Alexander & Crutcher, 1990; Alexander, DeLong, & Strick, 1986). The premotor circuits that connect the SMA, PMC, and ACC motor regions to the striatum and the thalamus include the putamen and the ventrolateral nuclei of the thalamus (Hatanaka et al., 2003; Alexander et al., 1986). The DLPFC circuit includes the caudate nucleus and the ventral anterior and dorsomedial nuclei of the thalamus (Alexander et al., 1986). In our study, basal ganglia activation included the bilateral caudate nucleus, putamen, and pallidum, whereas thalamic activation included the dorsomedial, ventrolateral, anterior, and ventral anterior nuclei. Therefore, speed emphasis resulted in distinct activity across both the premotor-related and the DLPFC-related cortico-striato-thalamo-cortical circuits that underlie the motor and context representations involved in this task.

Of particular interest is the fact that we found increased sustained activity under speed emphasis in the DLPFC, as we predicted on the basis of our PDP model. At first glance, this pattern of activation in the DLPFC might appear somewhat counterintuitive; in everyday speech, we typically treat emphasizing accuracy, paying closer attention, and “being careful” as more-or-less related concepts. However, our data appear to contradict

this notion. Our data are, in fact, consistent with the view that the DLPFC represents context (Miller & Cohen, 2001; Cohen et al., 1992) and has an excitatory influence on posterior representations (Egner & Hirsch, 2005; Miller & D'Esposito, 2005), because an area involved in executive control that provides top-down support to activate motor representations would be expected to display elevated activation during speed emphasis, which is what we found in the present study. This pattern of activation is also consistent with findings implicating a role for the DLPFC not just in task preparation (MacDonald, Cohen, Stenger, & Carter, 2000; Sohn, Ursu, Anderson, Stenger, & Carter, 2000) but also in movement preparation (Pochon et al., 2001).

Most of the regions whose baseline activity was modulated by SAT were also engaged by our PPI analyses, thus providing support for the notion that, in order to emphasize speed, the DLPFC provides an excitatory top-down control signal that increases the sustained baseline activity in these regions. Remarkably, a recent study by Egner and Hirsch (2005) used a similar analysis to show that the DLPFC provides a similar excitatory top-down control signal to sensory regions during increased perceptual attention. Our data are therefore consistent with the proposal that the DLPFC provides an excitatory biasing signal that engages task-relevant representations (Miller & Cohen, 2001). Thus, our data support the notion that the DLPFC controls SAT in a similar way as the context unit in our PDP model does.

It is important to note that the increased DLPFC activation under speed emphasis most likely does not constitute perceptual attention or selection, like it is thought to do in response to, or in anticipation of, difficult trials in interference tasks such as the Stroop task (Egner & Hirsch, 2005; MacDonald et al., 2000). This is because the Simon interference effect was greater under speed emphasis, whereas greater attention under speed emphasis would have predicted the opposite. Our PPI results also do not support this notion; no sensory areas were identified by these analyses, as would have been expected if the role of the DLPFC in this study was to resolve interference (Egner & Hirsch, 2005). Next, it could have been argued that the need for interference resolution might still be greater under speed emphasis and that the increased DLPFC activity still might reflect interference resolution. However, a median-split analysis showed that those with a greater loss in accuracy under speed emphasis also showed a greater increase in baseline activity in the DLPFC. This argues against the notion that the DLPFC region implied here is involved with overcoming conflict, as this would have predicted that a greater difference in DLPFC activity would have been associated with smaller performance impairment. This inverse relationship between activation and performance impairment has been found for DLPFC regions thought to be involved with preparing to overcome conflict (e.g., MacDonald et al., 2000). In contrast, the

positive relationship between DLPFC activity and performance impairment that we found is consistent with our notion that the DLPFC regulates SAT by increasing baseline activity. Finally, we note that DLPFC regions implicated in perceptual attention and preparing to overcome conflict are often situated more posteriorly than the regions identified in the current study (e.g., Barber & Carter, 2005; Weissman, Warner, & Woldorff, 2004; MacDonald et al., 2000).

A more general, though not inconsistent, interpretation of DLPFC function in SAT holds that the increased activity under speed emphasis reflects the control necessary to overcome a "default" or more automatic state of responding accurately, assuming that participants' natural tendency is to emphasize accuracy over speed. Furthermore, this view might also predict increased DLPFC activation with accuracy emphasis in situations or tasks in which the natural tendency is to emphasize speed more, and control would be needed to emphasize accuracy. For these reasons, it might be instructive to include a condition with no specific speed or accuracy emphasis in future studies, and to investigate SAT in different types of tasks.

Our results suggest a left lateralization of the implementation of SAT. This might be specific to the task participants were performing; alternatively, it might reflect the normal operation of SAT. Future studies of SAT should shed more light on these possibilities. It should, however, be noted that the left DLPFC region in our study is remarkably similar to a left DLPFC region recently implicated in integrating sensory evidence supporting perceptual decisions (Heekeren, Marrett, Ruff, Bandettini, & Ungerleider, 2006). The conclusion that the left DLPFC is also involved in regulating SAT fits very well in these data.

It could be argued that the greater BOLD responses under accuracy emphasis might simply be due to longer processing under accuracy emphasis; after all, RTs were longer in this condition. This would indeed be a confound if the effects we found were located in sensory regions. Single-cell recordings from monkeys have shown that sensory regions (such as area MT, a region dedicated to detecting motion) typically increase their firing rates when motion in the neuron's receptive field is in its preferred direction. However, these neurons only display a brief burst of activity, followed by a steady but noisy state of activity that does not change for the duration of the stimulus (Britten, Shadlen, Newsome, & Movshon, 1993); no accumulation-like pattern of activity is observed in this or other sensory regions. In contrast, an accumulation-like pattern of activation is typically observed in the parietal and premotor cortices, which are thought to represent the accumulation of evidence for one decision or another (Huk & Shadlen, 2005; Smith & Ratcliff, 2004; Gold & Shadlen, 2002; Roitman & Shadlen, 2002). Similarly, the lateralized readiness potential, which is thought to be generated by motor

and premotor cortices, also appears to represent an accumulation process (Spencer & Coles, 1999). Thus, we find it unlikely that the increased BOLD response under accuracy emphasis could represent an artifact of longer processing. It is more likely that it represents a greater distance between baseline and threshold. Note, however, that in the context of an evidence accumulator, processing time and neural activation are intrinsically confounded with one another. Future studies involving single-cell recordings in nonhuman primates that explicitly manipulate controlled SAT could shed further light on this issue.

It is possible that, in addition to a change in baseline activity, SAT is modulated by a change in threshold. This is, for instance, a core assumption random walk or diffusion models make to account for SAT (e.g., Bogacz et al., 2006; Ratcliff & Rouder, 1998). Computationally, a reduction in threshold to emphasize speed would be equivalent to an increase in baseline. Our data suggest that speed is emphasized by an increase in baseline and a reduction in the amount of neural evidence needed to reach threshold. Thus, our data do not address whether the change in baseline is accompanied by a decrease in threshold. The use of an uninstructed baseline condition in future studies might allow us to address this possibility. Additionally, future work involving single-cell recordings from nonhuman primates might also be able to clarify this particular issue.

The ability to trade speed and accuracy is an important aspect of our remarkable cognitive and behavioral flexibility; we can choose to focus on whatever mode of responding we judge to be more important given the situation. The present study has increased our understanding of these abilities by identifying the neural processes that underlie the ability to strategically control the position along the SAT continuum. Future research might focus on possible differences between tasks (Rinkenauer et al., 2004; Van der Lubbe et al., 2001), or on the neural basis of the role of reward rate in manipulating SAT (Simen et al., 2006; Gold & Shadlen, 2002)¹.

Acknowledgments

This research was supported by grants K02 MH64190, RO1 MH066629, and Burroughs-Wellcome 1002274.01, to C. S. C. Vincent van Veen is now at the Helen Wills Neuroscience Institute, UC Berkeley.

Reprint requests should be sent to Cameron S. Carter, Imaging Research Center, UC Davis Medical Center, 4711 X St., Sacramento, CA 95817, or via e-mail: cameron.carter@ucdmc.ucdavis.edu.

Note

1. The present article has dealt with the question of how we establish a desired level of SAT. The astute reader might wonder a further set of questions: Once we have established this desired SAT level, how does this modulate activation related to

conflict, errors, and trial-to-trial adjustments in control? An analysis of these data in these terms is forthcoming. In the meantime, the interested reader is referred to van Veen (2006).

REFERENCES

- Alexander, G. E., & Crutcher, M. D. (1990). Functional architecture of basal ganglia circuits: Neural substrates of parallel processing. *Trends in Neurosciences*, *13*, 266–271.
- Alexander, G. E., DeLong, M. R., & Strick, P. L. (1986). Parallel organization of functionally segregated circuits linking basal ganglia and cortex. *Annual Review of Neuroscience*, *9*, 357–381.
- Ball, T., Schreiber, A., Feige, B., Wagner, M., Lücking, C. H., & Kristeva-Feige, R. (1999). The role of higher-order motor areas in voluntary movement as revealed by high-resolution EEG and fMRI. *Neuroimage*, *10*, 682–694.
- Barber, A. D., & Carter, C. S. (2005). Cognitive control involved in overcoming prepotent response tendencies and switching between tasks. *Cerebral Cortex*, *15*, 899–912.
- Bogacz, R., Brown, E. T., Moehlis, J., Holmes, P., & Cohen, J. D. (2006). The physics of optimal decision making: A formal analysis of models of performance in two-alternative forced choice tasks. *Psychological Review*, *113*, 700–765.
- Britten, K., Shadlen, M., Newsome, W., & Movshon, J. (1993). Responses of neurons in macaque MT to stochastic motion signals. *Visual Neuroscience*, *10*, 1157–1169.
- Bunge, S. A., Hazeltine, E., Scanlon, M. D., Rosen, A. C., & Gabrieli, J. D. E. (2002). Dissociable contributions of prefrontal and parietal cortices to response selection. *Neuroimage*, *17*, 1562–1571.
- Churchland, M. M., Santhanam, G., & Shenoy, K. V. (2006). Preparatory activity in premotor and motor cortex reflects the speed of the upcoming reach. *Journal of Neurophysiology*, *96*, 3130–3146.
- Cohen, J. D., Dunbar, K., & McClelland, J. L. (1990). On the control of automatic processes: A parallel distributed processing account of the Stroop effect. *Psychological Review*, *97*, 332–361.
- Cohen, J. D., Servan-Schreiber, D., & McClelland, J. L. (1992). A parallel distributed processing approach to automaticity. *American Journal of Psychology*, *105*, 239–269.
- Craft, J. L., & Simon, J. R. (1970). Processing symbolic information from a visual display: Interference from an irrelevant directional cue. *Journal of Experimental Psychology*, *83*, 415–420.
- Desimone, R., & Duncan, J. (1995). Neural mechanisms of selective visual attention. *Annual Review of Neuroscience*, *18*, 193–222.
- Dosenbach, N. U. F., Visscher, K. M., Palmer, E. D., Miezin, F. M., Wenger, K. K., Kang, H. C., et al. (2006). A core system for the implementation of task sets. *Neuron*, *50*, 799–812.
- Egner, T., & Hirsch, J. (2005). Cognitive control mechanisms resolve conflict through cortical amplification of task-relevant information. *Nature Neuroscience*, *8*, 1784–1790.
- Friston, K. J., Buechel, C., Fink, G. R., Morris, J., Rolls, E., & Dolan, R. J. (1997). Psychophysiological and modulatory interactions in neuroimaging. *Neuroimage*, *6*, 218–229.
- Ghez, C. (1991). Voluntary movement. In E. R. Kandel, J. H. Schwartz, & T. M. Jessell (Eds.), *Principles of neural science* (3rd ed., pp. 609–625). Norwalk, CT: Appleton & Lange.
- Glover, G. H. (1999). Deconvolution of impulse response in event-related BOLD fMRI. *Neuroimage*, *9*, 416–429.
- Gold, J. I., & Shadlen, M. N. (2000). Representation of a perceptual decision in developing oculomotor commands. *Nature*, *404*, 390–394.

- Gold, J. I., & Shadlen, M. N. (2002). Banburismus and the brain: Decoding the relationship between sensory stimuli, decisions, and reward. *Neuron*, *36*, 299–308.
- Gratton, G., Coles, M. G., Sirevaag, E. J., Eriksen, C. W., & Donchin, E. (1988). Pre- and poststimulus activation of response channels: A psychophysiological analysis. *Journal of Experimental Psychology: Human Perception and Performance*, *14*, 331–344.
- Gratton, G., Coles, M. G. H., & Donchin, E. (1992). Optimizing the use of information: Strategic control of activation of responses. *Journal of Experimental Psychology: General*, *121*, 480–506.
- Graybiel, A. M., Aosaki, T., Flaherty, A. W., & Kimura, M. (1994). The basal ganglia and adaptive motor control. *Science*, *265*, 1826–1831.
- Grodd, W., Hülsmann, E., Lotze, M., Wildgruber, D., & Erb, M. (2001). Sensorimotor mapping of the human cerebellum: fMRI evidence of somatotopic organization. *Human Brain Mapping*, *13*, 55–73.
- Hanes, D. P., & Schall, J. D. (1996). Neural control of voluntary movement initiation. *Science*, *274*, 427–430.
- Hanks, T. D., Ditterich, J., & Shadlen, M. N. (2006). Microstimulation of macaque area LIP affects decision-making in a motion discrimination task. *Nature Neuroscience*, *9*, 682–689.
- Hatanaka, N., Tokuno, H., Hamada, I., Inase, M., Ito, Y., Imanishi, M., et al. (2003). Thalamocortical and intracortical connections of monkey cingulate motor areas. *Journal of Comparative Neurology*, *462*, 121–138.
- Heekeren, H. R., Marrett, S., Ruff, D. A., Bandettini, P. A., & Ungerleider, L. G. (2006). Involvement of the left dorsolateral prefrontal cortex in perceptual decision making is independent of response modality. *Proceedings of the National Academy of Sciences, U.S.A.*, *103*, 10023–10028.
- Huk, A. C., & Shadlen, M. N. (2005). Neural activity in macaque parietal cortex reflects temporal integration of visual motion signals during perceptual decision making. *Journal of Neuroscience*, *25*, 10420–10436.
- Lo, C.-C., & Wang, X.-J. (2006). Cortico-basal ganglia circuit mechanism for a decision threshold in reaction time tasks. *Nature Neuroscience*, *9*, 956–963.
- Luck, S. J., & Hillyard, S. A. (2000). The operation of selective attention at multiple stages of processing: Evidence from human and monkey electrophysiology. In M. S. Gazzaniga (Ed.), *The new cognitive neurosciences* (pp. 687–700). Cambridge: MIT Press.
- MacDonald, A. W., III, Cohen, J. D., Stenger, V. A., & Carter, C. S. (2000). Dissociating the role of the dorsolateral prefrontal and anterior cingulate cortex in cognitive control. *Science*, *288*, 1835–1838.
- Meyer, D. E., Irwin, D. E., Osman, A. M., & Kounios, J. (1988). The dynamics of cognition and action: Mental processes inferred from speed–accuracy decomposition. *Psychological Review*, *95*, 183–237.
- Miller, B. T., & D’Esposito, M. (2005). Searching for “the top” in top–down control. *Neuron*, *48*, 535–538.
- Miller, E. K., & Cohen, J. D. (2001). An integrative theory of prefrontal cortex function. *Annual Review of Neuroscience*, *24*, 167–202.
- Osman, A., Lou, L., Müller-Gethmann, H., Rinkenauer, G., Mattes, S., & Ulrich, R. (2000). Mechanisms of speed–accuracy tradeoff: Evidence from covert motor processes. *Biological Psychology*, *51*, 173–199.
- Pachella, R. G. (1974). The interpretation of reaction time in information-processing research. In B. H. Kantowitz (Ed.), *Human information processing: Tutorials in performance and recognition* (pp. 481–482). Hillsdale, NJ: Erlbaum.
- Picard, N., & Strick, P. L. (1996). Motor areas of the medial wall: A review of their location and functional activation. *Cerebral Cortex*, *6*, 342–353.
- Picard, N., & Strick, P. L. (2001). Imaging the premotor areas. *Current Opinion in Neurobiology*, *11*, 663–672.
- Pochon, J.-B., Levy, R., Poline, J.-B., Crozier, S., Lehericy, S., Pillon, B., et al. (2001). The role of dorsolateral prefrontal cortex in the preparation of forthcoming actions: An fMRI study. *Cerebral Cortex*, *11*, 260–266.
- Ratcliff, R., & Rouder, J. N. (1998). Modeling response times for two-choice decisions. *Psychological Science*, *9*, 347–356.
- Reddi, B. A. J., Asrress, K. N., & Carpenter, R. H. S. (2003). Accuracy, information, and response time in a saccadic decision task. *Journal of Neurophysiology*, *90*, 3538–3546.
- Reddi, B. A. J., & Carpenter, R. H. S. (2000). The influence of urgency on decision time. *Nature Neuroscience*, *3*, 827–830.
- Rinkenauer, G., Osman, A., Ulrich, R., Müller-Gethmann, H., & Mattes, S. (2004). On the locus of speed–accuracy tradeoff in reaction time: Inferences from the lateralized readiness potential. *Journal of Experimental Psychology: General*, *133*, 261–282.
- Roitman, J. D., & Shadlen, M. N. (2002). Response of neurons in the lateral intraparietal area during a combined visual discrimination reaction time task. *Journal of Neuroscience*, *22*, 9475–9489.
- Rumelhart, D. E., McClelland, J. L., & the PDP Research Group. (1986). *Parallel distributed processing: Explorations in the microstructure of cognition. Vol. 1: Foundations*. Cambridge: MIT Press.
- Rushworth, M. F. S., Krams, M., & Passingham, R. E. (2001). The attentional role of the left parietal cortex: The distinct lateralization and localization of motor attention in the human brain. *Journal of Cognitive Neuroscience*, *13*, 698–710.
- Rushworth, M. F. S., Paus, T., & Sipila, P. K. (2001). Attention systems and the organization of the human parietal cortex. *Journal of Neuroscience*, *21*, 5262–5271.
- Schall, J. D. (2003). Neural correlates of decision processes: Neural and mental chronometry. *Current Opinion in Neurobiology*, *13*, 182–186.
- Schall, J. D. (2004). On building a bridge between brain and behavior. *Annual Review of Psychology*, *55*, 23–50.
- Shadlen, M. N., & Newsome, W. T. (2001). Neural basis of a perceptual decision in the parietal cortex (area LIP) of the rhesus monkey. *Journal of Neurophysiology*, *86*, 1916–1936.
- Simen, P., Cohen, J. D., & Holmes, P. J. (2006). Rapid decision threshold modulation by reward rate in a neural network. *Neural Networks*, *19*, 1013–1026.
- Smith, P. L., & Ratcliff, R. (2004). Psychology and neurobiology of simple decisions. *Trends in Neurosciences*, *27*, 161–168.
- Snyder, L. H., Dickinson, A. R., & Calton, J. L. (2006). Preparatory delay activity in the monkey parietal reach region predicts reach reaction times. *Journal of Neuroscience*, *26*, 10091–10099.
- Sohn, M.-H., Ursu, S., Anderson, J. R., Stenger, V. A., & Carter, C. S. (2000). The role of prefrontal cortex and posterior parietal cortex in task switching. *Proceedings of the National Academy of Sciences, U.S.A.*, *97*, 13448–13453.
- Spencer, K. M., & Coles, M. G. H. (1999). The lateralized readiness potential: Relationship between human data and response activation in a connectionist model. *Psychophysiology*, *36*, 364–370.

- Strick, P. L. (2004). Basal ganglia and cerebellar circuits with the cerebral cortex. In M. S. Gazzaniga (Ed.), *The cognitive neurosciences* (3rd ed., pp. 453–461). Cambridge: MIT Press.
- Usher, M., & McClelland, J. L. (2001). The time course of perceptual choice: The leaky, competing accumulator model. *Psychological Review*, *108*, 550–592.
- Van der Lubbe, R. H. J., Jaśkowski, P., Wauschkuhn, B., & Verleger, R. (2001). Influence of time pressure in a simple response task, a choice-by-location task, and the Simon task. *Journal of Psychophysiology*, *15*, 241–255.
- van Veen, V. (2006). *A neuroimaging approach to the relationship between attention and speed–accuracy tradeoff*. Unpublished doctoral thesis, University of Pittsburgh, Pittsburgh, PA.
- Visscher, K. M., Miezin, F. M., Kelly, J. E., Buckner, R. L., Donaldson, D. I., McAvoy, M. P., et al. (2003). Mixed blocked/event-related designs separate transient and sustained activity in fMRI. *Neuroimage*, *19*, 1694–1708.
- Weissman, D. H., Warner, L. M., & Woldorff, M. G. (2004). The neural mechanisms for minimizing cross-modal distraction. *Journal of Neuroscience*, *24*, 10941–10949.
- Wickelgren, W. A. (1977). Speed–accuracy tradeoff and information processing dynamics. *Acta Psychologica*, *41*, 67–85.
- Zorzi, M., & Umiltà, C. (1995). A computational model of the Simon effect. *Psychological Research*, *58*, 193–205.